Gas Separation Hot Paper

How to cite: *Angew. Chem. Int. Ed.* **2022**, *61*, e202210343
International Edition: doi.org/10.1002/anie.202210343
German Edition: doi.org/10.1002/ange.202210343

A Metal-Organic Framework with Nonpolar Pore Surfaces for the One-Step Acquisition of C_2H_4 from a C_2H_4 and C_2H_6 Mixture

*Zhengyi Di[+], Caiping Liu[+], Jiandong Pang, Shuixiang Zou, Zhenyu Ji, Falu Hu, Cheng Chen, Daqiang Yuan, Maochun Hong, and Mingyan Wu**

Abstract: Because C_2H_4 plays an essential role in the chemical industry, economical and energy-efficient separation of ethylene (C_2H_4) from ethane (C_2H_6) is extremely important. With the exception of energy-intensive cryogenic distillation, there are few one-step methods to obtain polymer-grade ($\geq$99.95 % pure) C_2H_4 from C_2H_4/C_2H_6 mixtures. Here we report a highly stable metal-organic-framework (MOF) FJI-H11-Me-(des) (FJI-H = Hong's group in Fujian Institute of Research on the Structure of Matter) which features one-dimensional hexagonal nonpolar pore surfaces constructed by aromatic rings and alkyl groups. This FJI-H11-Me(des) adsorbs C_2H_6 rather than C_2H_4 between 273 and 303 K. Practical breakthrough experiments with C_2H_4 containing 1 % C_2H_6 have shown that FJI-H11-Me(des) can realize the acquisition in one-step of polymer-grade, 99.95 % pure C_2H_4 under various conditions including different gas flow rates, temperatures and relative humidity.

Introduction

As an important raw material to produce polyethylene, polyvinyl chloride, synthetic rubber, and other organic chemical products, ethylene (C_2H_4) will have an annual global production capacity of more than 200 million tons in 2023 and maintains an annual growth trend of about 5 %.[1] In industry, steam cracking or thermal decomposition of ethane (C_2H_6) is an important method to produce ethylene,[2] but the C_2H_4 produced in this way contains a small amount of residual C_2H_6. The production of pure ethylene is one of the most important processes in the industrial repertoire.[2e,3] Separation of C_2H_4 and C_2H_6 however is challenging owing to their very similar physicochemical properties and molecular size ($3.28\times4.18\times4.84$ Å^3 and $3.81\times4.08\times4.82$ Å^3 for C_2H_4 and C_2H_6, respectively). Currently, the industrial separation of C_2H_4 from C_2H_6 is typically achieved by cryogenic distillation at high pressure and low temperature. This process is energy-intensive however due to the very close boiling points of C_2H_4 and C_2H_6, and requires very large distillation columns with 120 to 180 trays and high reflux ratios. Usually, the total worldwide energy consumption of this process is about 800 PJ per year, which is more than 0.3 % of annual global energy consumption.[4] Therefore, efficient separation of C_2H_4 and C_2H_6 is of great significance to reduce worldwide energy consumption.[5]

Recently, efficient and convenient adsorptive separation processes based on porous materials have attracted increasing attention.[6] Some adsorbents, such as zeolite, metal-organic frameworks (MOFs) and other crystalline materials, have been developed for C_2H_4/C_2H_6 separation.[2b,6b,7] Since the C_2H_4 molecule has a larger quadrupole moment (1.50×10^{-26} esu cm^2) than C_2H_6 (0.65×10^{-26} esu cm^2),[8] most of the current adsorbents adsorb C_2H_4 preferentially over C_2H_6,[9] due to the stronger interactions between the C_2H_4 molecule and the open metal sites or clusters. Consequently, an additional desorption process is required to release the C_2H_4 gas absorbed in the porous materials,[10] and this consumes much energy and prolongs the separation procedure. Due to the common co-adsorption phenomenon, it is also difficult to obtain polymer-grade ($\geq$99.95 %) C_2H_4 through one adsorption-desorption cycle.[3a,11] In order to obtain C_2H_4 in a one-step process, the development of new porous materials which adsorb C_2H_6 preferentially is necessary. Since the polarizability surface of C_2H_4 (42.52×10^{-25} cm^3) is lower than that of C_2H_6 (44.7×10^{-25} cm^3), the nonpolar pore surfaces of porous materials, which are typically comprised of aromatic or aliphatic moieties, may afford a substantial energy contribution to the preferential adsorption of C_2H_6 over C_2H_4.[12] Using the above porous materials as adsorbents, one-step acquisition of C_2H_4 from C_2H_4 and C_2H_6 mixture can be realized. However, at present the construction of C_2H_6-selective MOFs is still a difficult problem.[13]

With the above considerations in mind, we have designedly synthesized a tetracarboxylic ligand with six phenyl rings as the skeleton and methyl groups as substituents. A flexible porous framework with NbO topology can be obtained when assembled with classical paddlewheel dicopper(II) units.[14] With the loss of solvent molecules, the flexible framework will contract gradually and the dinuclear

[*] Dr. Z. Di,[+] Dr. C. Liu,[+] Prof. Dr. J. Pang, S. Zou, Z. Ji, Dr. F. Hu, Dr. C. Chen, Prof. Dr. D. Yuan, Prof. Dr. M. Hong, Prof. Dr. M. Wu
State Key Lab of Structure Chemistry, Fujian Institute of Research on the Structure of Matter, Chinese Academy of Sciences
Fuzhou, Fujian 350002 (China)
E-mail: wumy@fjirsm.ac.cn
Dr. Z. Di[+]
College of Chemistry, Tianjin Key Laboratory of Structure and Performance for Functional Molecules, Tianjin Normal University
Tianjin, 300387 (China)
[+] These authors contributed equally to this work.

Cu^{II} units may be shielded by the organic ligands, resulting in a nonpolar pore surface decorated with aromatic phenyl and aliphatic methyl groups. As a result, these nonpolar pores will be helpful not only to preferentially capture C_2H_6 over C_2H_4 but also to improve the humid stability of the framework due to the hydrophobic surface of the channel.[15] As anticipated, we developed a highly stable copper-organic framework with nonpolar pore surfaces (Figure 1a). In this structure, the methyl groups of the ligands are arrayed in an orderly fashion along a one-dimensional hexagonal channel and are directed into the center of the channel. Thus, the methyl groups, together with phenyl rings of the organic ligands constitute a nonpolar pore surface, while the Cu^{II} ions are shielded by the aromatic rings and have no access to gas molecules. Due to this unique nonpolar pore structure, this porous material exhibits as anticipated, delivering preferential adsorption of C_2H_6 over C_2H_4 at ambient temperature and pressure. Experiments have shown that high-pure C_2H_4 ($\geq$99.95 % pure) be obtained by this material directly from C_2H_6/C_2H_4 mixtures containing 1 % C_2H_6. The porous material described here retains its excellent separation performance under various conditions including different gas flow rates, temperatures and relative humidity.

Results and Discussion

FJI-H11-Me can be obtained as blue-green crystals from the solvothermal reaction of $Cu(NO_3)_2{\cdot}3H_2O$ with the designed synthetic tetracarboxylic ligand (Figures S1 and S2).[14] The as-synthesized sample was changed with low boiling solvents for 3 days and were then heated at 80 °C for 10 h in dynamic vacuum to obtain the solvent-free FJI-H11-Me (termed FJI-H11-Me(des)). Single crystal X-ray diffraction experiments show that FJI-H11-Me(des) crystallizes in monoclinic space group *C*2/m (CCDC No. 2189349, as shown in Table S1),[16] and constructed with fully deprotonated tetracarboxylic ligands and classical dinuclear Cu^{II} units (See Figures S3 and S4). Each dinuclear Cu^{II} unit is connected to only four carboxylic groups and there are no solvent molecules on the axial sites, which distinguishes it from the coordination modes of the classical dinuclear Cu^{II} units.[17] A unique feature of FJI-H11-Me(des) is that the unsaturated dinuclear Cu^{II} units are shielded by the phenyl rings and the separation between Cu^{II} ions and the centers of the phenyl rings is 3.06 Å (Figure S5). As a result, the Cu^{II} ions have no access to guest molecules. Upon packing, there are two kinds of pores, the hexagonal pore A and the triangular pore B, along the *c* axis in FJI-H11-Me(des). As seen in Figures 1a, b and S6, the hexagonal pores are connected with each other to form a one-dimensional channel, while the triangular pores B are discrete. On the wall of channel A, the ligand is obliquely arranged and the methyl group of the ligand is directed into the center of channel A to form the nonpolar pore surfaces (Figure S7).

The gas adsorption capacity of FJI-H11-Me(des) was studied with an N_2 isotherm at 77 K and a CO_2 isotherm at 195 K (Figure 1c), indicating an obvious breathing behavior. The N_2 isotherm exhibits a step at 43 kPa and CO_2 isotherm exhibits a step at 54 kPa and these can be assigned to the structural transformation from the state with small pores

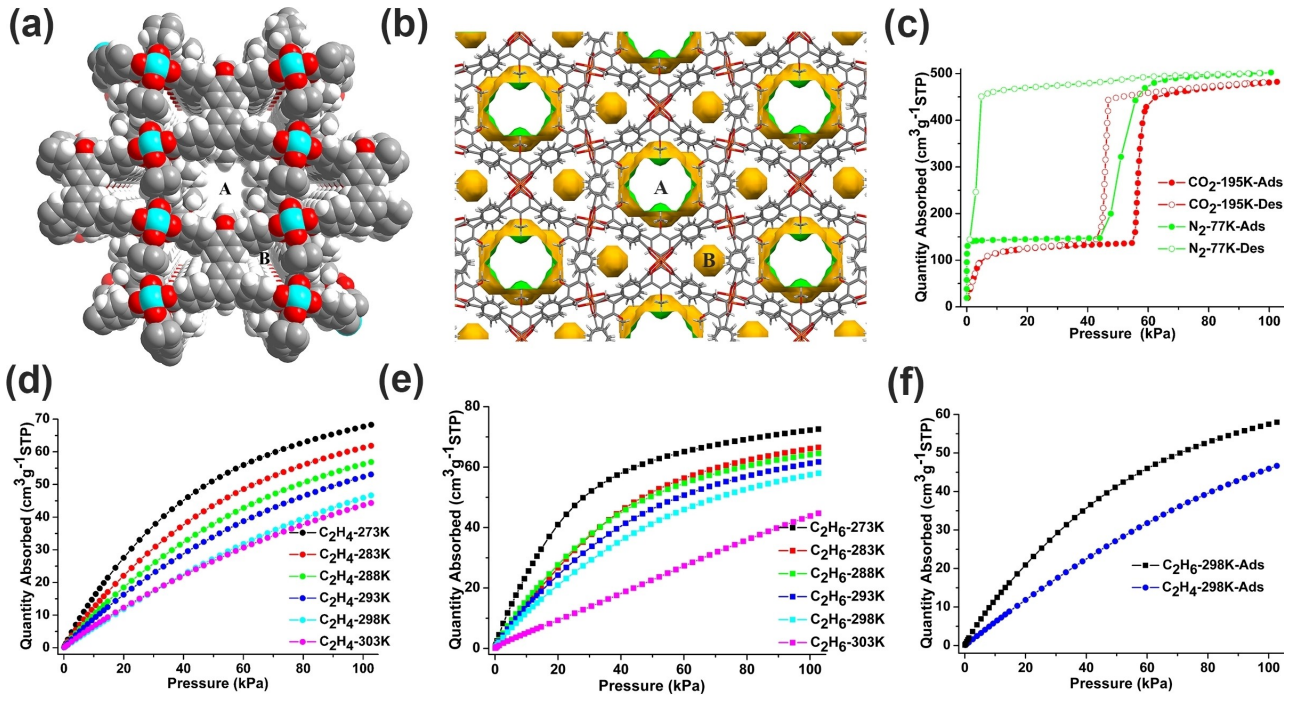

Figure 1. a) and b) One-dimensional channels (A and B) in desolvated FJI-H11-Me along the *c* axis. c) Single-component sorption isotherms of N_2 at 77 K and CO_2 at 195 K for desolvated FJI-H11-Me. d) and e) Single-component adsorption isotherms of C_2H_4 and C_2H_6 at 273, 283, 288, 293, 298 and 303 K respectively. f) The comparison of adsorption isotherms of C_2H_4 and C_2H_6 at 298 K.

changing to a state with large pores.[18] There are also obvious hysteresis loops upon desorption. These results indicate that FJI-H11-Me(des) has some structural flexibility. To study the potential of FJI-H11-Me(des) for separation applications, single-component adsorption isotherms of C_2H_4 and C_2H_6 at 273, 283, 288, 293, 298 and 303 K were performed (Figures 1d and e) to evaluate the potential in the separation of a binary C_2H_6/C_2H_4 mixture at ambient temperature and pressure.[19] As shown in Figures 1d and e, the C_2H_6 adsorption capacity of FJI-H11-Me(des) is much higher than that of C_2H_4 at the same temperature, implying the stronger affinity of FJI-H11-Me(des) for C_2H_6.[20] At 298 K, the maximum uptakes for C_2H_6 and C_2H_4 are 57.97 $cm^3 g^{-1}$ and 46.65 $cm^3 g^{-1}$, respectively. Further tests at 298 K indicate there is no obvious decrease in C_2H_4 and C_2H_6 uptakes after three adsorption-desorption cycles (Figures S9 and S10). FJI-H11-Me(des) was exposed to the atmosphere for 2 or 7 days, and then the adsorption tests for C_2H_4 and C_2H_6 were repeated. The results showed that the adsorption amounts did not experience a significant decrease (Figures S11 and S12), which indicates that FJI-H11-Me(des) has high moisture stability. Such high stability is comparable to other famous MOFs such as TIFSIX-3-Ni[21] and Azole-Th-1[22] (Table S2).

The heats of adsorption (Q_{st}) of C_2H_6 and C_2H_4 on FJI-H11-Me(des) were calculated from the isotherms at 273, 298 and 303 K. The values of Q_{st} for C_2H_6 and C_2H_4 were calculated to be 38.9 kJ mol^{-1} (Figure S14) and 25.9 kJ mol^{-1} respectively (Figure S15) at zero coverage, which indicates the stronger interactions between FJI-H11-Me(des) and C_2H_6 than those for C_2H_4 molecules.[23] Ideal adsorbed solution theory (IAST) calculations were performed to estimate the adsorption selectivity of C_2H_6/C_2H_4 (1:99) for FJI-H11-Me(des). As we can see from the Figure S16, the adsorption selectivity of C_2H_6/C_2H_4 (1:99) is 2.09, which is larger than developed MOF materials such as NUM-9a (1.62)[24] or TJT-100 (1.2)[25] Overall, FJI-H11-Me(des) affords a large C_2H_6/C_2H_4 uptake ratio of 124 % and the adsorption heat (Q_{st}) ratio of C_2H_6/C_2H_4 for FJI-H11-Me(des) was calculated to be 150 %. The above results are consistent with FJI-H11-Me(des) realizing one-step C_2H_6/C_2H_4 separation.

In order to estimate the actual gas separation achievement of FJI-H11-Me(des), we performed the experiments in a packed column of activated FJI-H11-Me(des) to evaluate its separation performance with actual 1/99 C_2H_6/C_2H_4 mixtures. First, we removed solvent molecules from the surface of the sample with a vacuum pump for 2 h. Then the sample was placed in a stainless-steel tube and activated at 80 °C for about 10 h to completely remove the solvent molecules. As can be seen in Figure 2a, FJI-H11-Me(des) can effectively separate C_2H_6/C_2H_4 (v/v, 1/99) gas mixtures with the gas flow rates of 1 mL min^{-1}. C_2H_4 gas passes through the adsorption bed first at ca. 41 min to directly yield polymer-grade C_2H_4 (≥ 99.95 % pure) gas with an undetectable amount of C_2H_6 (the detection limit of the instrument is 100 ppm). In contrast, the C_2H_6 gas can be detected by GC at ca. 50 min, due to the stronger force between the ethane molecules and FJI-H11-Me(des). In order to examine the separation performance of FJI-H11-Me(des) under ambient conditions, the recycling experiments were also carried out. As shown in Figure 2a, the breakthrough performance remains almost unchanged during three continuous cycles, confirming its good recycling ability for C_2H_6/C_2H_4 separation. We also tested the separation ability of FJI-H11-Me(des) at different gas flow rates (1, 1.5 and 2 mL min^{-1}) (Figure 2b) and different temperatures (298, 303, 308 and 313 K) (Figure 2c). The above tests indicate that FJI-H11-Me(des) can still realize the one-step separation of the C_2H_6/C_2H_4 mixture. From the breakthrough curves, we can see that FJI-H11-Me(des) adsorbs both C_2H_4 and C_2H_6 simultaneously. The simulated diffusion energy barrier for C_2H_6 is found to be 93.2 kJ mol^{-1} in the one-dimensional hexagonal channel of FJI-H11-Me-(des), which is significantly greater than the value of 24.3 kJ mol^{-1} for C_2H_4 (Figure S18). The simulation results showed that the larger-sized C_2H_6 is more favorably adsorbed. Therefore, the separation is likely thermodynamically driven. In order to simulate the humid environment in a practical situation, we also tested the C_2H_6/C_2H_4 separation performance of FJI-H11-Me(des) at conditions with different relative humidity (RH). As can be seen in Figure 2d, the separation performance showed no obvious change in the range of 33–100 % RH. The separation time persists at a gas flow rate of 1 mL min^{-1}, which indicates that the humidity has no obvious effect on the C_2H_6/C_2H_4 separation performance. It was concluded that the excellent C_2H_6/C_2H_4 separation performance of FJI-H11-Me(des) is due to the hydrophobic nonpolar pore surfaces, which have stronger interactions with C_2H_6 than with C_2H_4.

In order to identify the sites of the interaction between gas molecules and the framework of FJI-H11-Me(des), we performed Grand Canonical Monte Carlo (GCMC) simulations. As anticipated, C_2H_6 interacts with the pore surfaces of FJI-H11-Me(des) and has multiple supramolecular interactions as shown in Figure 3a. There are seven C–H···π interactions between the H atoms of C_2H_6 and the phenyl rings of the ligands with the H···π separations from 3.485 to 4.920 Å.[26] There are also four C–H···O interactions (H···O separations from 3.361 to 4.096 Å)[27] as well as a C···C interaction (C···C separation, 4.122 Å).[25,28] In comparison, there are fewer supramolecular interactions between C_2H_4 and the pore surfaces of FJI-H11-Me(des). There are only four C–H···π interactions (H···π separations, from 3.318 to 4.718 Å), two C–H···O interactions (H···O separations, 3.258 and 3.992 Å) and a C···C interaction (C···C separation, 4.125 Å) (Figure 3b). For C_2H_6, the calculated static binding energy is 62.70 kJ mol^{-1}, which is higher than that of C_2H_4 (55.74 kJ mol^{-1}). The difference between the static binding energy for C_2H_6 and C_2H_4 is 6.96 kJ mol^{-1}, indicating that FJI-H11-Me(des) prefers to adsorb C_2H_6 over C_2H_4, promising good performance for C_2H_6/C_2H_4 separation. The above results indicate the nonpolar pore surface favors adsorption of C_2H_6 rather than C_2H_4.

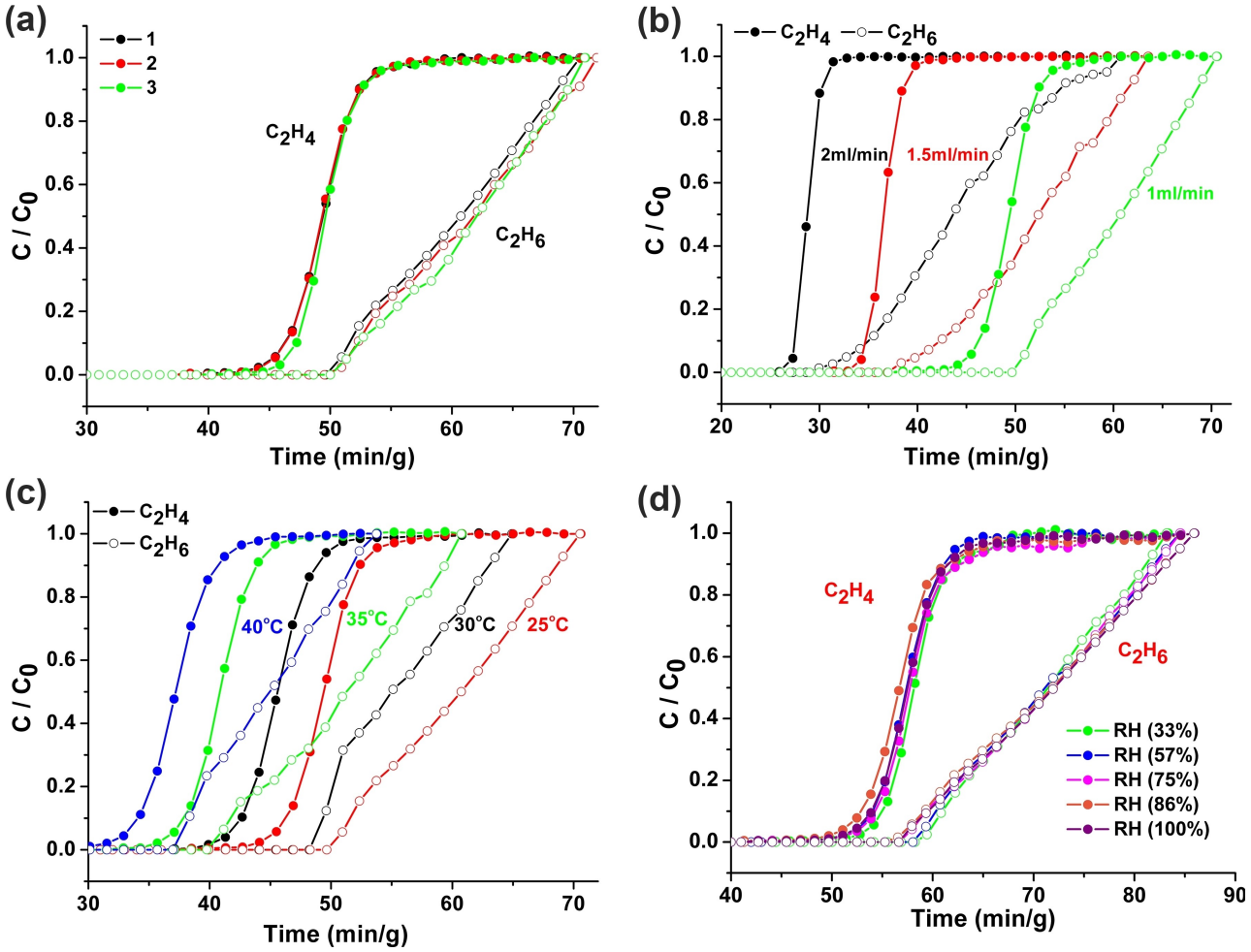

Figure 2. Experimental column breakthrough curves for a C_2H_6/C_2H_4 (v/v, 1/99) mixture in an absorber bed packed with FJI-H11-Me(des) at 298 K and 1 bar. a) The cycling breakthrough experiment tests of FJI-H11-Me(des) (1 mL min^{-1}). b) An experiment with FJI-H11-Me(des) under different gas flow rates (black 2 mL min^{-1}, red 1.5 mL min^{-1}, green 1 mL min^{-1}). c) The experiment of FJI-H11-Me(des) under different temperatures with gas flow rate of the 1 mL min^{-1} (red 25 °C, black 30 °C, green 35 °C, blue 40 °C). d) The experiment of FJI-H11-Me(des) under different relative humidity with gas flow rate of the 1 mL min^{-1}.

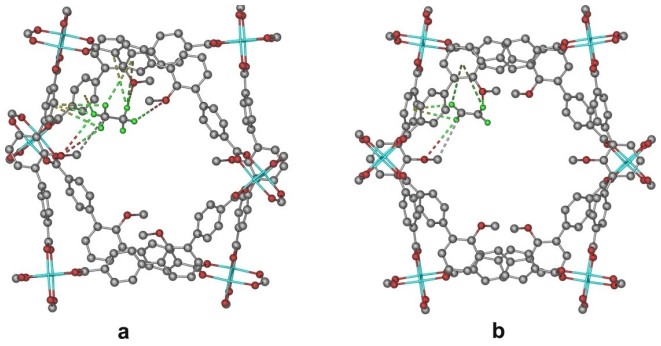

Figure 3. Schematic adsorption sites for a) C_2H_6 and b) C_2H_4 obtained from theoretical calculations. For clarity, the hydrogen atoms of the ligands are omitted and the hydrogen atoms of C_2H_6 and C_2H_4 are in green. The dashed lines show the weak interactions between the gas molecule and the pore surface.

Conclusion

We report a stable metal-organic framework with one-dimensional hexagonal nonpolar aromatic pore surfaces constructed by aromatic rings and alkyl groups. Due to this unique nonpolar pore structure, FJI-H11-Me(des) as anticipated, prefers to adsorb C_2H_6 rather than C_2H_4 over a wide range of temperatures. Experiments conducted under ambient conditions show that >99.95 % pure C_2H_4 can be obtained directly from mixtures containing 1 % C_2H_6. More importantly, FJI-H11-Me(des) retains good separation performance at different gas flow rates, temperatures, and relative humid conditions. The above results indicate that the nonpolar pore surfaces can realize one-step acquisition of pure C_2H_4 from C_2H_4/C_2H_6 mixtures.

Acknowledgements

We acknowledge the financial supports of National Nature Science Foundation of China (21871266), Fujian Science & Technology Innovation Laboratory for Optoelectronic Information of China (No. 2021ZR120), Nature Science Foundation of Fujian Province (No. 2021J01517 and 2020J06034), Youth Innovation Promotion Association CAS. The microcrystal diffraction of FJI-H11-Me(des) was carried out with the assistance of Prof. Yu-Sheng Chen at NSF's ChemMatCARS. NSF's ChemMatCARS Sector 15 is principally supported by the Divisions of Chemistry (CHE) and Materials Research (DMR), National Science Foundation, under grant number NSF/CHE-1834750. Use of the Advanced Photon Source, an Office of Science User Facility operated for the U.S. Department of Energy (DOE) Office of Science by Argonne National Laboratory, was supported by the U.S. DOE under Contract No. DE-AC02-06CH11357. We thank Dr. Wei Chen (Innovation Academy for Precision Measurement Science and Technology, CAS) for the calculation of diffusion barriers.

Conflict of Interest

The authors declare no conflict of interest.

Data Availability Statement

The data that support the findings of this study are available in the Supporting Information of this article.

Keywords: C_2H_4/C_2H_6 Separation · Gas Adsorption · Humidity · Metal-Organic Frameworks · Nonpolar Pore Surfaces

[1] a) D. S. Sholl, R. P. Lively, *Nature* **2016**, *532*, 435–437; b) A. Corma, E. Corresa, Y. Mathieu, L. Sauvanaud, S. Al-Bogami, M. S. Al-Ghrami, A. Bourane, *Catal. Sci. Technol.* **2017**, *7*, 12–46; c) F. Bander, http://seperationtechnology.com/; d) J. Y. S. Lin, *Science* **2016**, *353*, 121–122; e) L. Li, R. B. Lin, R. Krishna, H. Li, S. Xiang, H. Wu, J. Li, W. Zhou, B. Chen, *Science* **2018**, *362*, 443–446.

[2] a) H. Yang, Y. Wang, R. Krishna, X. Jia, Y. Wang, A. N. Hong, C. Dang, H. E. Castillo, X. Bu, P. Feng, *J. Am. Chem. Soc.* **2020**, *142*, 2222–2227; b) B. Zhu, J.-W. Cao, S. Mukherjee, T. Pham, T. Zhang, T. Wang, X. Jiang, K. A. Forrest, M. J. Zaworotko, K.-J. Chen, *J. Am. Chem. Soc.* **2021**, *143*, 1485–1492; c) R. B. Lin, L. Li, H. L. Zhou, H. Wu, C. He, S. Li, R. Krishna, J. Li, W. Zhou, B. Chen, *Nat. Mater.* **2018**, *17*, 1128–1133; d) S. M. Kuznicki, V. A. Bell, S. Nair, H. W. Hillhouse, R. M. Jacubinas, C. M. Braunbarth, B. H. Toby, M. Tsapatsis, *Nature* **2001**, *412*, 720–724; e) L. Yang, S. Qian, X. Wang, X. Cui, B. Chen, H. Xing, *Chem. Soc. Rev.* **2020**, *49*, 5359–5406.

[3] a) R.-B. Lin, S. Xiang, H. Xing, W. Zhou, B. Chen, *Coord. Chem. Rev.* **2019**, *378*, 87–103; b) C.-X. Chen, Z.-W. Wei, T. Pham, P. C. Lan, L. Zhang, K. A. Forrest, S. Chen, A. M. Al-Enizi, A. Nafady, C.-Y. Su, S. Ma, *Angew. Chem. Int. Ed.* **2021**, *60*, 9680–9685; *Angew. Chem.* **2021**, *133*, 9766–9771; c) Z. Jiang, L. Fan, P. Zhou, T. Xu, S. Hu, J. Chen, D.-L. Chen, Y. He, *Inorg. Chem. Front.* **2021**, *8*, 1243–1252.

[4] a) M. H. Mohamed, Y. Yang, L. Li, S. Zhang, J. P. Ruffley, A. G. Jarvi, S. Saxena, G. Veser, J. K. Johnson, N. L. Rosi, *J. Am. Chem. Soc.* **2019**, *141*, 13003–13007; b) F. Jin, E. Lin, T. Wang, S. Geng, T. Wang, W. Liu, F. Xiong, Z. Wang, Y. Chen, P. Cheng, Z. Zhang, *J. Am. Chem. Soc.* **2022**, *144*, 5643–5652.

[5] a) S. Chu, Y. Cui, N. Liu, *Nat. Mater.* **2017**, *16*, 16–22; b) R. Vaidhyanathan, S. S. Iremonger, G. K. H. Shimizu, P. G. Boyd, S. Alavi, T. K. Woo, *Science* **2010**, *330*, 650–653; c) J. W. Yoon, H. Chang, S. J. Lee, Y. K. Hwang, D. Y. Hong, S. K. Lee, J. S. Lee, S. Jang, T. U. Yoon, K. Kwac, Y. Jung, R. S. Pillai, F. Faucher, A. Vimont, M. Daturi, G. Ferey, C. Serre, G. Maurin, Y. S. Bae, J. S. Chang, *Nat. Mater.* **2017**, *16*, 526–531; d) J. Pei, K. Shao, L. Zhang, H. M. Wen, B. Li, G. Qian, *Top. Curr. Chem.* **2019**, *377*, 2–34; e) X. Guo, S. Geng, M. Zhuo, Y. Chen, M. J. Zaworotko, P. Cheng, Z. Zhang, *Coord. Chem. Rev.* **2019**, *391*, 44–68; f) Y. P. Li, Y. N. Zhao, S. N. Li, D. Q. Yuan, Y. C. Jiang, X. Bu, M. C. Hu, Q. G. Zhai, *Adv. Sci.* **2021**, *8*, 2003141; g) L. Li, R. B. Lin, R. Krishna, X. Wang, B. Li, H. Wu, J. Li, W. Zhou, B. Chen, *J. Am. Chem. Soc.* **2017**, *139*, 7733–7736; h) Y. Chai, X. Han, W. Li, S. Liu, S. Yao, C. Wang, W. Shi, I. da-Silva, P. Manuel, Y. Cheng, L. D. Daemen, A. J. Ramirez-Cuesta, C. C. Tang, L. Jiang, S. Yang, N. Guan, L. Li, *Science* **2020**, *368*, 1002–1006.

[6] a) Z. Di, C. Liu, J. Pang, C. Chen, F. Hu, D. Yuan, M. Wu, M. Hong, *Angew. Chem. Int. Ed.* **2021**, *60*, 10828–10832; *Angew. Chem.* **2021**, *133*, 10923–10927; b) K. J. Chen, D. G. Madden, S. Mukherjee, T. Pham, K. A. Forrest, A. Kumar, B. Space, J. Kong, Q. Y. Zhang, M. J. Zaworotko, *Science* **2019**, *366*, 241–246; c) X. W. Gu, J. X. Wang, E. Wu, H. Wu, W. Zhou, G. Qian, B. Chen, B. Li, *J. Am. Chem. Soc.* **2022**, *144*, 2614–2623; d) P. Zhou, L. Yue, X. Wang, L. Fan, D. L. Chen, Y. He, *ACS Appl. Mater. Interfaces* **2021**, *13*, 54059–54068; e) W. Fan, S. Yuan, W. Wang, L. Feng, X. Liu, X. Zhang, X. Wang, Z. Kang, F. Dai, D. Yuan, D. Sun, H. C. Zhou, *J. Am. Chem. Soc.* **2020**, *142*, 8728–8737; f) L. Gong, Y. Ye, Y. Liu, Y. Li, Z. Bao, S. Xiang, Z. Zhang, B. Chen, *ACS Appl. Mater. Interfaces* **2022**, *14*, 19623–19628; g) Y.-Y. Xue, X.-Y. Bai, J. Zhang, Y. Wang, S.-N. Li, Y.-C. Jiang, M.-C. Hu, Q.-G. Zhai, *Angew. Chem. Int. Ed.* **2021**, *60*, 10122–10128; *Angew. Chem.* **2021**, *133*, 10210–10216; h) Q. Dong, X. Zhang, S. Liu, R. B. Lin, Y. Guo, Y. Ma, A. Yonezu, R. Krishna, G. Liu, J. Duan, R. Matsuda, W. Jin, B. Chen, *Angew. Chem. Int. Ed.* **2020**, *59*, 22756–22762; *Angew. Chem.* **2020**, *132*, 22944–22950; i) S. Chen, N. Behera, C. Yang, Q. Dong, B. Zheng, Y. Li, Q. Tang, Z. Wang, Y. Wang, J. Duan, *Nano Res.* **2021**, *14*, 546–553; j) Z. Di, J. Pang, F. Hu, M. Wu, M. Hong, *Nano Res.* **2021**, *14*, 2584–2588; k) Y. Jiang, J. Hu, L. Wang, W. Sun, N. Xu, R. Krishna, S. Duttwyler, X. Cui, H. Xing, Y. Zhang, *Angew. Chem. Int. Ed.* **2022**, *61*, e202200947; *Angew. Chem.* **2022**, *134*, e202200947; l) L. Li, L. Guo, D. H. Olson, S. Xian, Z. Zhang, Q. Yang, K. Wu, Y. Yang, Z. Bao, Q. Ren, J. Li, *Science* **2022**, *377*, 335–339.

[7] a) A. A. Lysova, D. G. Samsonenko, K. A. Kovalenko, A. S. Nizovtsev, D. N. Dybtsev, V. P. Fedin, *Angew. Chem. Int. Ed.* **2020**, *59*, 20561–20567; *Angew. Chem.* **2020**, *132*, 20742–20748; b) M. Kang, D. W. Kang, J. H. Choe, H. Kim, D. W. Kim, H. Park, C. S. Hong, *Chem. Mater.* **2021**, *33*, 6193–6199; c) H. Zeng, M. Xie, T. Wang, R.-J. Wei, X.-J. Xie, Y. Zhao, W. Lu, D. Li, *Nature* **2021**, *595*, 542–548; d) H. Furukawa, K. E. Cordova, M. O'Keeffe, O. M. Yaghi, *Science* **2013**, *341*, 1230444; e) P. Q. Liao, N. Y. Huang, W. X. Zhang, J. P. Zhang, X. M. Chen, *Science* **2017**, *356*, 1193–1196; f) M. Chang, J. Ren, Q. Yang, D. Liu, *Chem. Eng. J.* **2021**, *408*, 127294.

[8] a) R. S. Pillai, M. L. Pinto, J. Pires, M. Jorge, J. R. Gomes, *ACS Appl. Mater. Interfaces* **2015**, *7*, 624–637; b) G.-D. Wang, Y.-Z. Li, W.-J. Shi, L. Hou, Y.-Y. Wang, Z. Zhu, *Angew. Chem. Int. Ed.* **2022**, *61*, e202205427; *Angew. Chem.* **2022**, *134*, e202205427.

[9] a) Y. Yang, L. Li, R. B. Lin, Y. Ye, Z. Yao, L. Yang, F. Xiang, S. Chen, Z. Zhang, S. Xiang, B. Chen, *Nat. Chem.* **2021**, *13*, 933–939; b) S. Yang, A. J. Ramirez-Cuesta, R. Newby, V. Garcia-Sakai, P. Manuel, S. K. Callear, S. I. Campbell, C. C. Tang, M. Schroder, *Nat. Chem.* **2015**, *7*, 121–129.

[10] a) L. Yang, L. Yan, W. Niu, Y. Feng, Q. Fu, S. Zhang, Y. Zhang, L. Li, X. Gu, P. Dai, D. Liu, Q. Zheng, X. Zhao, *Angew. Chem. Int. Ed.* **2022**, *61*, e202204046; *Angew. Chem.* **2022**, *134*, e202204046; b) J. Liu, J. Miao, S. Ullah, K. Zhou, L. Yu, H. Wang, Y. Wang, T. Thonhauser, J. Li, *ACS Mater. Lett.* **2022**, *4*, 1227–1232.

[11] Y. Wang, C. Hao, W. Fan, M. Fu, X. Wang, Z. Wang, L. Zhu, Y. Li, X. Lu, F. Dai, Z. Kang, R. Wang, W. Guo, S. Hu, D. Sun, *Angew. Chem. Int. Ed.* **2021**, *60*, 11350–11358; *Angew. Chem.* **2021**, *133*, 11451–11459.

[12] G.-D. Wang, J. Chen, Y.-Z. Li, L. Hou, Y.-Y. Wang, Z. Zhu, *Chem. Eng. J.* **2022**, *433*, 133786.

[13] a) S. Wang, Q. Yang, C. Zhong, *Sep. Purif. Technol.* **2008**, *60*, 30–35; b) P. Q. Liao, W. X. Zhang, J. P. Zhang, X. M. Chen, *Nat. Commun.* **2015**, *6*, 8697; c) X.-Q. Wu, J.-H. Liu, T. He, P.-D. Zhang, J. Yu, J.-R. Li, *Chem. Eng. J.* **2021**, *407*, 127183; d) L. Li, L. Guo, S. Pu, J. Wang, Q. Yang, Z. Zhang, Y. Yang, Q. Ren, S. Alnemrat, Z. Bao, *Chem. Eng. J.* **2019**, *358*, 446–455.

[14] J. Pang, C. Liu, Y. Huang, M. Wu, F. Jiang, D. Yuan, F. Hu, K. Su, G. Liu, M. Hong, *Angew. Chem. Int. Ed.* **2016**, *55*, 7478–7482; *Angew. Chem.* **2016**, *128*, 7604–7608.

[15] S. Ullah, K. Tan, D. Sensharma, N. Kumar, S. Mukherjee, A. A. Bezrukov, J. Li, M. J. Zaworotko, T. Thonhauser, *Angew. Chem. Int. Ed.* **2022**, *61*, e202206613; *Angew. Chem.* **2022**, *134*, e202206613.

[16] Deposition Number 2189349 contains the supplementary crystallographic data for this paper. These data are provided free of charge by the joint Cambridge Crystallographic Data Centre and Fachinformationszentrum Karlsruhe Access Structures service.

[17] a) J. Pang, F. Jiang, M. Wu, C. Liu, K. Su, W. Lu, D. Yuan, M. Hong, *Nat. Commun.* **2015**, *6*, 7575; b) S. S. Y. Chui, S. M. F. Lo, J. P. H. Charmant, A. G. Orpen, I. D. Williams, *Science* **1999**, *283*, 1148–1150.

[18] a) J. A. Mason, J. Oktawiec, M. K. Taylor, M. R. Hudson, J. Rodriguez, J. E. Bachman, M. I. Gonzalez, A. Cervellino, A. Guagliardi, C. M. Brown, P. L. Llewellyn, N. Masciocchi, J. R. Long, *Nature* **2015**, *527*, 357–361; b) P. Lama, L. J. Barbour, *J. Am. Chem. Soc.* **2018**, *140*, 2145–2150; c) Z. Niu, Z. Fan, T. Pham, G. Verma, K. A. Forrest, B. Space, P. K. Thallapally, A. M. Al-Enizi, S. Ma, *Angew. Chem. Int. Ed.* **2022**, *61*, e202117807; *Angew. Chem.* **2022**, *134*, e202117807.

[19] R. Lyndon, W. You, Y. Ma, J. Bacsa, Y. Gong, E. E. Stangland, K. S. Walton, D. S. Sholl, R. P. Lively, *Chem. Mater.* **2020**, *32*, 3715–3722.

[20] a) O. T. Qazvini, R. Babarao, Z. L. Shi, Y. B. Zhang, S. G. Telfer, *J. Am. Chem. Soc.* **2019**, *141*, 5014–5020; b) X. W. Lei, H. Yang, Y. Wang, Y. Wang, X. Chen, Y. Xiao, X. Bu, P. Feng, *Small* **2021**, *17*, 2003167.

[21] A. Kumar, C. Hua, D. G. Madden, D. O'Nolan, K. J. Chen, L. J. Keane, J. J. Perry, M. J. Zaworotko, *Chem. Commun.* **2017**, *53*, 5946–5949.

[22] Z. Xu, X. Xiong, J. Xiong, R. Krishna, L. Li, Y. Fan, F. Luo, B. Chen, *Nat. Commun.* **2020**, *11*, 3163.

[23] J. G. Min, K. C. Kemp, S. B. Hong, *Sep. Purif. Technol.* **2020**, *250*, 117146.

[24] S. Q. Yang, F. Z. Sun, P. Liu, L. Li, R. Krishna, Y. H. Zhang, Q. Li, L. Zhou, T. L. Hu, *ACS Appl. Mater. Interfaces* **2021**, *13*, 962–969.

[25] H. G. Hao, Y. F. Zhao, D. M. Chen, J. M. Yu, K. Tan, S. Ma, Y. Chabal, Z. M. Zhang, J. M. Dou, Z. H. Xiao, G. Day, H. C. Zhou, T. B. Lu, *Angew. Chem. Int. Ed.* **2018**, *57*, 16067–16071; *Angew. Chem.* **2018**, *130*, 16299–16303.

[26] a) X. Zhang, L. Li, J. X. Wang, H. M. Wen, R. Krishna, H. Wu, W. Zhou, Z. N. Chen, B. Li, G. Qian, B. Chen, *J. Am. Chem. Soc.* **2020**, *142*, 633–640; b) Y. Ye, S. Xian, H. Cui, K. Tan, L. Gong, B. Liang, T. Pham, H. Pandey, R. Krishna, P. C. Lan, K. A. Forrest, B. Space, T. Thonhauser, J. Li, S. Ma, *J. Am. Chem. Soc.* **2022**, *144*, 1681–1689.

[27] X. Zhang, J.-X. Wang, L. Li, J. Pei, R. Krishna, H. Wu, W. Zhou, G. Qian, B. Chen, B. Li, *Angew. Chem. Int. Ed.* **2021**, *60*, 10304–10310; *Angew. Chem.* **2021**, *133*, 10392–10398.

[28] D. Antypov, A. Shkurenko, P. M. Bhatt, Y. Belmabkhout, K. Adil, A. Cadiau, M. Suyetin, M. Eddaoudi, M. J. Rosseinsky, M. S. Dyer, *Nat. Commun.* **2020**, *11*, 6099.

Manuscript received: July 14, 2022
Accepted manuscript online: August 17, 2022
Version of record online: August 31, 2022